THE PERFORMANCE OF MULTICHANNEL ADAPTIVE EQUALIZATION FOR LOS DIGITAL COMMUNICATION CORRUPTED BY INTERFERENCE

Michael Reuter, Richard North and James Zeidler

NCCOSC RDT&E Division
San Diego, CA 92152
reuter@nosc.mil

ABSTRACT

Multichannel adaptive equalization combines the concepts of spatial diversity and temporal equalization to improve receiver performance in a line-of-sight communication environment. In this paper, we derive the optimal Wiener filter for conditions common to this environment. We specifically analyze the effect of a CW interference on this solution and demonstrate the dependence of receiver performance on the MAEQ spatial-temporal beampattern.

1. INTRODUCTION

Multichannel adaptive equalization is a technique that combines the spatial processing of narrowband adaptive beamforming (ABF) with the temporal processing of single channel adaptive equalizers (AEQ) into a single joint spatial-temporal filter. The multichannel adaptive equalizer (MAEQ) is capable of compensating for intersymbol interference (ISI) induced by both finite bandwidth and dispersive communication channels while simultaneously mitigating the effects of flat channel fading and/or spatially correlated interference. It is a potentially important technique for improving the performance and reliability of line-of-sight (LOS) digital communication systems.

The MAEQ filter shown in Fig. 1 was origniated by Monsen [1, 2]. It has demonstrated significant performance improvements over narrowband ABFs and single channel AEQs in a variety of operating environments [3, 4, 5, 6, 7, 8, 9, 10, 11]. The structure consists of M antennas each followed by a two-sided fractionally-spaced equalizer (FSE) with oversampling factor O_s with N_1 leading and N_2 lagging taps, and an N_3-tap T-spaced decision feedback equalizer (DFE). The weights can be determined by any number of algorithms, many based on minimizing the mean square error (MMSE).

In this paper, we analyze the steady-state performance of the MAEQ for simultaneous multipath fading and additive interference. These conditions are common to high-data-rate LOS digital communication systems where the interference is often unintentional narrowband AM or FM voice. It will be shown that the MAEQ forms a narrowband spatial-temporal notch centered in the direction of propagation of the interferer and at the interferer frequency by exploiting the spatial-temporal correlation in the interferer. The steady-state solution is important because it is used in an analysis technique in which the dynamic weights of the MAEQ are decomposed into a Wiener filter term and a time-varying misadjustment term whose characteristics depend on the weight update equation. This is an

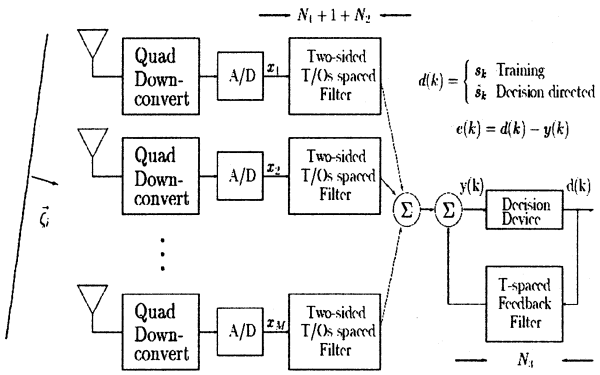

Figure 1: Multichannel adaptive equalizer.

established technique which offers insight into the adaptive process [12] [13].

The rest of this paper is organized as follows. In section 2, we define the signal and channel models used in this paper. Section 3 contains the derivation of the optimal Wiener weights of the MAEQ. We formulate the second-order statistics represented in the Wiener solution in a convenient matrix format in section 4. In section 5, we derive an approximate solution to the Wiener weights for the case of CW interference and no multipath. We show in section 6 that this approximation describes the dependence of the interference cancellation properties of the MAEQ on its spatial-temporal filter characteristics. These results are important for determining the number of antennas, the array geometry, and the number of MAEQ weights (N_1, N_2, N_3) for optimum performance. Future work will study the effects of the misadjustment filter and the interference bandwidth on the performance of the MAEQ.

2. SIGNAL AND CHANNEL MODELS

In this paper, we assume the signal propagates along L spatially separate channels from a single transmit antenna to each of M receive antennas. The baseband signal received at the m^{th} antenna can be written as

$$x_m(t) = \sum_{l=1}^{L} \beta_{m,l}(t) s(t - \vec{\alpha_l} \cdot \vec{p_m} - \Delta_{m,l}) \; e^{-j2\pi f_c(\vec{\alpha_l} \cdot \vec{p_m})} e^{-j2\pi f_c \Delta_{m,l}} + i(\vec{p_m}, t) + n_m(t) \quad (1)$$

where $s(t) = \sqrt{S} \sum_k s_k P_T(t - kT)$, and $i(\vec{p_m}, t) = i(t - \vec{\alpha_i} \cdot \vec{p_m}) e^{-j2\pi f_c(\vec{\alpha_i} \cdot \vec{p_m})}$. $\vec{p_m}$ is the coordinate vector of the

m^{th} sensor, $\vec{\alpha_l} = \vec{\zeta_l}/c$ is the propagation vector of the l^{th} path where $\vec{\zeta_l}$ is a unit vector which points in the direction of propagation and c is the speed of propagation, $\Delta_{m,l}$ is multipath delay of the l^{th} path, $\beta_{m,l}(t)$ is the fading component modeled as a zero mean, complex Gaussian process with autocorrelation function $\phi_{m,l}(\tau)$, f_c is the carrier frequency, $\{s_k\}$ is the sequence of transmitted symbols which are modeled as zero mean with unit variance and statistically independent, S is the signal power, and $P_T(t)$ is the combined baseband impulse response of the transmit and receive filters. $i(\vec{p_m}, t)$ is interference which is considered to be spatially correlated while $n_m(t)$ is the receiver noise assumed to be spatially and temporally uncorrelated with power spectral density σ_n^2. In general, $i(\vec{p_m}, t)$ will also arrive at the receiver via multiple paths, however for notational simplicity it is expressed as a lump sum in Eq. 1.

The interferer at the input to the equalizers is modeled as an ideal, bandpass, wide sense stationary process with power spectral density [13] [7]

$$P_i(f) = \begin{cases} N_B & f_\Delta - \frac{B}{2} \le f \le f_\Delta + \frac{B}{2} \\ 0 & \text{otherwise} \end{cases} \quad (2)$$

and autocorrelation function

$$\phi_i(\tau) = N_B B \text{sinc}(\pi B \tau) e^{j2\pi f_\Delta \tau}, \quad (3)$$

where f_Δ is the carrier offset frequency of the interferer. If we let $B \to 0$ so that $N_B B \to J$, we get a CW interference with autocorrelation function

$$\phi_i(\tau) = J e^{j2\pi f_\Delta \tau}. \quad (4)$$

3. WIENER SOLUTION

The Wiener solution to the MAEQ coefficients is best derived using a matrix formulation. In the following analysis, we assume ideal symbol decisions and synchronization. Define the equalizer tap coefficient vector of the m^{th} antenna as

$$\mathbf{a}_m(k) = [a_{m,-N_1}(k), ..., a_{m,0}(k), ..., a_{m,N_2}(k)]^T \quad (5)$$

and the baseband signal samples at the taps of the m^{th} equalizer to be

$$\mathbf{x}_m(k) = [x_m(kT + N_1 T/O_s), ..., x_m(kT), ..., x_m(kT - N_2 T/O_s)]^T. \quad (6)$$

Let c_l be the length of the filter impulse response $P_T(k)$ in samples of spacing $\frac{T}{O_s}$. Also, let

$$d_1 = \lfloor \frac{1}{O_s} \left(N_1 + \frac{c_l - 1}{2} \right) \rfloor, \quad d_2 = \lfloor \frac{1}{O_s} \left(N_2 + \frac{c_l - 1}{2} \right) \rfloor \quad (7)$$

where $\lfloor c \rfloor$ denotes the greatest integer less than or equal to c, and $d = d_1 + d_2 + 1$. Then $\mathbf{x}_m(k)$ can be represented in terms of its components as

$$\mathbf{x}_m(k) = \sum_{l=1}^{L} \beta_{m,l}(t) \mathbf{T}_{m,l}^H \mathbf{s}(k) + \mathbf{i}_m(k) + \mathbf{n}_m(k) \quad (8)$$

where the direct path is represented by path $l = 1$. $\mathbf{T}_{m,l}$ is an $d \times (N_1 + N_2 + 1)$ matrix in which each row is a replica of $\sqrt{S} P_T^*(\frac{kT}{O_s} - \vec{\alpha_l} \cdot \vec{p_m} - \Delta_{m,l}) e^{-j2\pi f_c (\vec{\alpha_l} \cdot \vec{p_m})} e^{-j2\pi f_c \Delta_{m,l}}$ time delayed by O_s samples with respect to the previous row and truncated by the observation window $N_1 + N_2 + 1$ [14]. $\mathbf{s}(k)$ is the corresponding vector of symbols in which the $d_1 + 1$ element corresponds to $d(k)$, the current symbol to be decoded. $\mathbf{i}_m(k)$ and $\mathbf{n}_m(k)$ are the interference and noise vectors respectively.

Next, we define the column vectors $vec(\mathbf{X}(k)) = [\mathbf{x}_1^T(k), ..., \mathbf{x}_M^T(k)]^T$ and $vec(\mathbf{A}(k)) = [\mathbf{a}_1^T(k), ..., \mathbf{a}_M^T(k)]^T$. Letting $\mathbf{b}(k)$ represent the feedback coefficient vector and $\mathbf{d}(k) = [d(k-1), ..., d(k-N_3)]$ the vector of N_3 previously decoded symbols, we can then write the output of the MAEQ as

$$y(k) = \mathbf{w}^H(k) \mathbf{f}(k) \quad (9)$$

where $\mathbf{w}(k) = [vec(\mathbf{A}(k))^T \ , \ \mathbf{b}^T(k)]^T$ and $\mathbf{f}(k) = [vec(\mathbf{X}(k))^T \ , \ \mathbf{d}^T(k)]^T$.

Using the principle of orthogonality, $E[(d(k) - y(k))^* \mathbf{f}(k)] = \mathbf{0}$, with the above expressions, it can be shown that

$$\begin{bmatrix} \mathbf{R} & \mathbf{Q}^H \\ \mathbf{Q} & \mathbf{I} \end{bmatrix} \begin{bmatrix} vec(\mathbf{A}^{opt}) \\ \mathbf{b}^{opt} \end{bmatrix} = \begin{bmatrix} \mathbf{p} \\ \mathbf{0} \end{bmatrix} \quad (10)$$

where $\mathbf{R}$=$E[vec(\mathbf{X}(k)) vec(\mathbf{X}(k))^H]$, $\mathbf{Q}$=$E[\mathbf{d}(k) vec(\mathbf{X}(k))^H]$ and $\mathbf{p}$=$E[d^*(k) vec(\mathbf{X}(k))]$. From Eq. 10, the Wiener solution to the M parallel FSEs is found to be

$$vec(\mathbf{A}^{opt}) = \left(\mathbf{R} - \mathbf{Q}^H \mathbf{Q} \right)^{-1} \mathbf{p} \quad (11)$$

and the Wiener solution to the decision feedback filter is found to be

$$\mathbf{b}^{opt} = -\mathbf{Q} vec(\mathbf{A}^{opt}). \quad (12)$$

The minimum mean square error of $d(k) - y(k)$ is then given by

$$\text{MMSE} = 1 - vec^H(\mathbf{A}^{opt}) \mathbf{p}. \quad (13)$$

Note that the effects of the DFE are implicitly included in the MMSE through $\mathbf{A}^{opt}$ of Eq. 11. The spatial-temporal beampattern is found from Eq. 22 of [7].

4. SECOND-ORDER STATISTICS

In this section, we assume that the direct path has no fading component and that it is incident broadside to the array ($\vec{\alpha_1} \cdot \vec{p_m} = 0$). In addition, we assume synchronization to the direct path so that we can set $\Delta_{m,1} = 0$ without loss of generality. In this case, let $\mathbf{T}_{m,1} = \mathbf{T}_s$ for all m and we decompose $\mathbf{T}_s$ into three components as

$$\mathbf{T}_s = \begin{bmatrix} \mathbf{E} \\ \mathbf{Q}_s \\ \mathbf{F} \end{bmatrix} \quad (14)$$

where $\mathbf{E}$ has $d_1 + 1$ rows and $\mathbf{Q}_s$ has $d_3 = \min(N_3, d_2)$ nonzero rows [14]. Then $\mathbf{Q} = \mathbf{1}_{1,M} \otimes \mathbf{Q}_s$ where $\mathbf{1}_{1,M}$ is a row vector of ones and $\otimes$ denotes Kroneker product. Then, let

$$\hat{\mathbf{T}}_s = \begin{bmatrix} \mathbf{E} \\ \mathbf{F} \end{bmatrix} \quad (15)$$

and $\hat{\mathbf{T}} = \mathbf{1}_{1,M} \otimes \hat{\mathbf{T}}_s$. Then

$$\mathbf{R} - \mathbf{Q}^H\mathbf{Q} = \hat{\mathbf{T}}^H\hat{\mathbf{T}} + \mathbf{D} + \sigma_n^2\mathbf{I} + \mathbf{\Psi} \tag{16}$$

where $\mathbf{D}$ is a block diagonal matrix whose m^{th} block component is $\sum_{l=2}^{L} \mathbf{\Phi}_{m,l} \odot \mathbf{T}_{m,l}^H \mathbf{T}_{m,l}$, where $\odot$ denotes element-wise product and $\mathbf{\Phi}_{m,l}$ is the covariance matrix of the l^{th} fading process at the m^{th} antenna [14]. Also, $\mathbf{p} = \mathbf{1}_{M,1} \otimes \mathbf{p}^s$ where $\mathbf{p}^s = [P_T(\frac{N_1 T}{O_s}), ...P_T(0), ..., P_T(\frac{-N_2 T}{O_s})]^T$.

$\mathbf{\Psi}$ is the interference covariance matrix which we can decompose as

$$\mathbf{\Psi} = \begin{bmatrix} \mathbf{\Psi}_{1,1} & \mathbf{\Psi}_{1,2} & \dots & \mathbf{\Psi}_{1,M} \\ \cdot & \cdot & \cdot & \cdot \\ \cdot & \cdot & \cdot & \cdot \\ \cdot & \cdot & \cdot & \cdot \\ \mathbf{\Psi}_{M,1} & \mathbf{\Psi}_{M,2} & \dots & \mathbf{\Psi}_{M,M} \end{bmatrix}. \tag{17}$$

Each block component is Toeplitz where, for the general broadband interferer,

$$\mathbf{\Psi}_{a,b}(i,j) = N_B B \text{sinc}\left(\pi B\left((i-j)\frac{T}{O_s} - \vec{\alpha_i}\cdot(\vec{p_a} - \vec{p_b})\right)\right) e^{j2\pi f_\Delta (i-j)\frac{T}{O_s}} e^{-j2\pi(f_c+f_\Delta)(\vec{\alpha_i}\cdot(\vec{p_a}-\vec{p_b}))} \tag{18}$$

We can simplify Eq. 17 for the CW interference by defining $\mathbf{i}_m = [e^{j2\pi f_\Delta \frac{N_1}{O_s}T}, ..., e^{-j2\pi f_\Delta \frac{N_2}{O_s}T}]^T e^{-j2\pi\vec{\alpha_i}\cdot\vec{p_m}(f_c+f_\Delta)}$. Then $\mathbf{\Psi} = J\mathbf{i}\mathbf{i}^H$ where $\mathbf{i} = [\mathbf{i}_1^T, \mathbf{i}_2^T, ..., \mathbf{i}_M^T]^T$.

5. CW INTERFERENCE ANALYSIS

In this section, we determine analytically the Wiener solution of the MAEQ for the CW interferer with no multipath components ($L = 1, \mathbf{D} = \mathbf{0}$).

We first use Eq. 16 in Eq. 11 and use the matrix inversion lemma (MIL) to get

$$vec(\mathbf{A}^{opt}) = \mathbf{B}^{-1}\mathbf{p} - \frac{J\mathbf{i}^H\mathbf{B}^{-1}\mathbf{p}}{1 + J\mathbf{i}^H\mathbf{B}^{-1}\mathbf{i}}\mathbf{B}^{-1}\mathbf{i} \tag{19}$$

where $\mathbf{B} = \hat{\mathbf{T}}^H\hat{\mathbf{T}} + \sigma_n^2\mathbf{I}$. Again invoking MIL we get

$$\mathbf{B}^{-1} = \frac{1}{\sigma_n^2}\left[\mathbf{I} - \frac{1}{\sigma_n^2}\hat{\mathbf{T}}^H\left(\mathbf{I}_{d-d_3} + \frac{M}{\sigma_n^2}\hat{\mathbf{T}}_s\hat{\mathbf{T}}_s^H\right)^{-1}\hat{\mathbf{T}}\right] \tag{20}$$

where $\hat{\mathbf{T}}_s\hat{\mathbf{T}}_s^H = \begin{bmatrix} \mathbf{E}\mathbf{E}^H & \mathbf{E}\mathbf{F}^H \\ \mathbf{F}\mathbf{E}^H & \mathbf{F}\mathbf{F}^H \end{bmatrix}$.

To continue the analysis we will make some simplifying assumptions. Let $N_1 = N_2 = N$, i.e., we have symetric two-sided equalizers, and $N_3 = d_2 = \frac{d-1}{2}$ so that $\hat{\mathbf{T}}_s = \mathbf{E}_{\frac{d+1}{2},2N+1}$. In order to analytically invert Eq. 20 we will make the approximation that $\mathbf{E}\mathbf{E}^H \approx \|\mathbf{p}^s\|^2\mathbf{I}_{\frac{d+1}{2}}$, i.e., that shifted versions of the filter impulse response are mutually orthogonal. This approximation is very good for symmetric filter impulse responses with the majority of the temporal support in a narrow region about the center of the response as is the case for the commonly-used raised cosine pulse. We then get

$$\mathbf{B}^{-1} \approx \frac{1}{\sigma_n^2}\left[\mathbf{I} - \frac{1}{\sigma_n^2 + M\|\mathbf{p}^s\|^2}\mathbf{1}_{M,M} \otimes \mathbf{E}^H\mathbf{E}\right] \tag{21}$$

We then use this approximation of $\mathbf{B}^{-1}$ to find the components of Eq. 19 [14]. Defining the system impulse response in vector form as $\mathbf{h} = [P_T(1), ..., P_T(c_l)]^T$ with Fourier transform $H(e^{j2\pi f_\Delta \frac{T}{O_s}})$ and

$$\rho = \sum_{m=1}^{M} e^{-j2\pi(f_\Delta + f_c)\vec{\alpha_i}\cdot\vec{p_m}} \tag{22}$$

$$\gamma = \frac{J}{\sigma_n^2}/[MS\|h\|^2 + \sigma_n^2 + \frac{J}{\sigma_n^2}[M(MS\|h\|^2 + \sigma_n^2)(2N+1) - \frac{\|\rho\|^2}{O_s}S\|H(e^{j2\pi f_\Delta \frac{T}{O_s}})\|^2(N+1)]] \tag{23}$$

we get, for the m^{th} equalizer, for $-N \le n \le 0$,

$$a_{m,n}^{opt} \approx \frac{1}{SM\|\mathbf{h}\|^2 + \sigma_n^2}p_n^s - \gamma\rho^*\sqrt{S}H^*(e^{j2\pi f_\Delta \frac{T}{O_s}}) \left[e^{-j2\pi(f_\Delta + f_c)\vec{\alpha_i}\cdot\vec{p_m}} - \frac{S\frac{\rho}{O_s}\|H(e^{j2\pi f_\Delta \frac{T}{O_s}})\|^2}{SM\|\mathbf{h}\|^2 + \sigma_n^2}\right] e^{-j2\pi f_\Delta n\frac{T}{O_s}} \tag{24}$$

and for $1 \le n \le N$ we get

$$a_{m,n}^{opt} \approx \frac{1}{SM\|\mathbf{h}\|^2 + \sigma_n^2}p_n^s - \gamma\rho^*\sqrt{S}H^*(e^{j2\pi f_\Delta \frac{T}{O_s}}) e^{-j2\pi(f_\Delta + f_c)\vec{\alpha_i}\cdot\vec{p_m}} e^{-j2\pi f_\Delta n\frac{T}{O_s}} \tag{25}$$

where we recognize the first component of Eq. 24 and 25 to be the matched filter term.

We can now use Eq. 12 to find the DFE coefficients. Define $h_c(n)$ as the convolution of the filter impulse response with itself. Then let $\mathbf{h}_d = [h_c(c_l + O_s), h_c(c_l + 2O_s), ..., h_c(c_l + \frac{d-1}{2}O_s)]^T$ and $d_4 = \lfloor\frac{N}{O_s}\rfloor$. Then we can show that [14]

$$b_n^{opt} \approx \frac{-M}{SM\|h\|^2 + \sigma_n^2}h_{d,n} + \gamma\|\rho\|^2 S \|H^*(e^{j2\pi f_\Delta \frac{T}{O_s}})\|^2 e^{-j2\pi f_\Delta nT} \quad 1 \le n \le d_4 \tag{26}$$

Finally, the MMSE is determined to be

$$\text{MMSE} \approx \frac{\sigma_n^2\left(1 + \|\rho\|^2 S\|H(e^{j2\pi f_\Delta \frac{T}{O_s}})\|^2\gamma\right)}{\sigma_n^2 + MS\|\mathbf{h}\|^2} \tag{27}$$

We note that $\|\rho\|^2$ is the conventional narrowband beampattern of the antenna array evaluated in the direction $\vec{\zeta_i}$ at frequency $f_\Delta + f_c$.

6. SIMULATION

In this section, we demonstrate the utility of the previous analytical results. As a measure of performance we use excess MMSE (EMMSE) in which we subtract the MMSE obtained at the MAEQ output *without* interference (set $\gamma = 0$ in Eq 27) from the MMSE resulting *with* interference. We simulate a scenario in which the desired signal with center frequency $f_c = 300$MHz ($\lambda = 1m$) and symbol duration $T = 1/1.544$MHz is incident broadside to a vertical, evenly-spaced array with four antennas, $O_s = 2$, and $N = 30$. The transmit filter is a square-root raised cosine pulse with 30% excess bandwidth and $c_l = 23$. The CW interference has offset frequency $f_\Delta = 154.4$KHz. SNR = 0dB and SIR = -20dB. In Fig. 2, we plot the spatial-temporal beampattern of the MAEQ with the interferer at 50^o elevation.

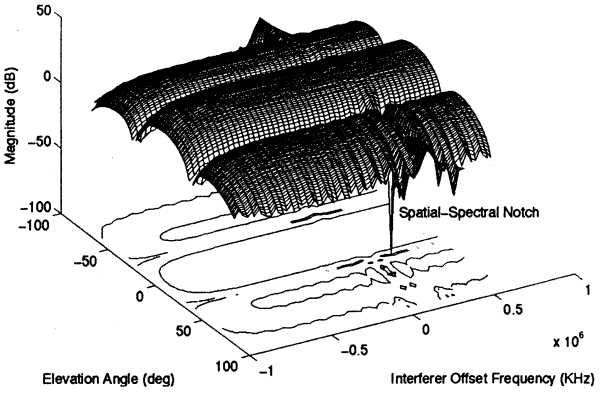

Figure 2: Beampattern for MAEQ with $M = 4$ and $N = 30$ with an interferer at 50^o elevation.

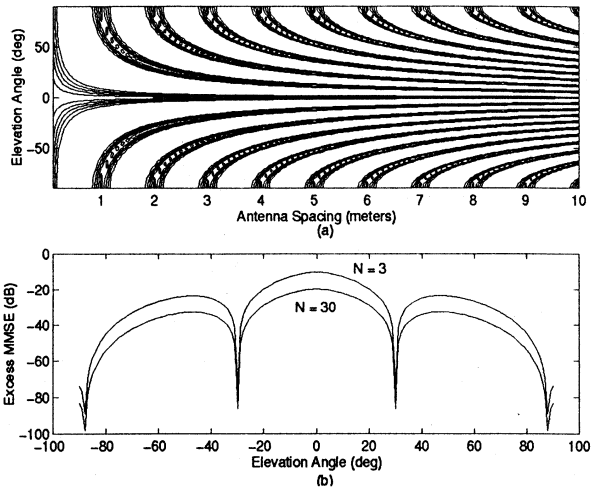

Figure 3: (a) Contour plot of EMMSE for interference elevation angle versus antenna spacing, $M = 4$ and $N = 30$ (b) EMMSE versus interference elevation angle for .5m ($\lambda/2$) spacing for $N = 3$ and $N = 30$.

The approximate Wiener solutions of Eqs. 24, 25 and 26 were found to agree closely with the simulations and with the exact, numerically-generated coefficients obtained using Eqs. 11 and 12. A narrowband notch is seen to be centered at the interferer effectively cancelling it both spatially and spectrally. Figure 3(a) is a plot of EMMSE for various interference elevation angles versus antenna spacing. We clearly see the characteristic spatial aliasing problem associated with evenly-spaced line arrays. Figure 3(b) is a plot of EMMSE versus interference elevation angle for .5m ($\lambda/2$) spacing and for two equalizer lengths. The effect of finite filter length on EMMSE is observed. Notice that the regions where the EMMSE of the $N = 3$ structure matches that of the $N = 30$ correspond to deep nulls in the beampattern. From Figs. 2 and 3, the relationship between EMMSE and the spatial-temporal beampattern becomes apparent.

7. CONCLUSION

In this paper, we derived the Wiener solution for a multichannel adaptive, fractionally-spaced equalizer with decision feedback. We additionally established an approximation of the Wiener solution for a CW interference and demonstrated how the filter coefficients and the MMSE are dependent on the MAEQ spatial-temporal beampattern. Analysis of the general broadband interferer proceeds similarly to that of the CW interference. Also, work is progressing to use these analytical results to estimate probability of symbol errors for various array configurations and propagation environments [14].

8. REFERENCES

[1] P. Monsen. High speed digital communication receiver. United States Patent Number 3,879,664, 1975.

[2] P. Monsen. Theoretical and measured performance of a DFE modem on a fading multipath channel. *IEEE Trans. on Comm.*, COM-25(10):1144–1153, Oct. 1977.

[3] M. Stojanovic, J. Catipovic, and J Proakis. An algorithm for multichannel coherent digital communications over long range underwater acoustic telemetry channels. In *Proc. IEEE Oceans-92*, 1992.

[4] J. Winters, J. Salz, and R. Gitlin. The impact of antenna diversity on the capacity of wireless communications systems. *IEEE Trans. Commun.*, 42(2/3/4):1740–1751, February/March/April 1994.

[5] Q. Wen and J. Ritcey. Spatial diversity equalization applied to underwater communications. *IEEE J. Oceanic Eng.*, 19(2):227–241, April 1994.

[6] M. Clark, L. Greenstein, W. Kennedy, and M. Shafi. Optimum linear diversity receivers for mobile communications. *IEEE Trans. on Vehicular Tech.*, VT-43(1):47–56, February 1994.

[7] R. North and J. Zeidler. Multichannel adaptive equalization for improved performance in LOS digital radio. In *1994 IEEE MILCOM*, 1994.

[8] S. Buljore and J. F. Diouris. A theoretical study of a multisensor equalizer using the MSE for the radiomobile channel (GSM model). In *28th ASILOMAR Conf. on Signals, Systems and Computers*, 1994.

[9] R. Gooch and B. Sublett. Joint spatial and temporal equalization in a decision directed adaptive antenna system. In *22th ASILOMAR Conf. on Signals, Systems and Computers*, pages 255–259, 1988.

[10] K. Scott and S. Nichols. Antenna diversity with multichannel adaptive equalization in digital radio. In *Proc. Int. Conf. on Comm.*, pages 1463–1468, 1991.

[11] N. Lo, D. Falconer, and A. Sheikh. Adaptive equalization and diversity combining for mobile radio using interpolated channel estimates. *IEEE Trans. on Vehicular Tech.*, VT-40(3):636–645, August 1991.

[12] J. Rickard and J. Zeidler. Second-order output statistics of the adaptive line enhancer. *IEEE Trans. on ASSP*, ASSP-27(1):31–39, February 1979.

[13] R. North, R. Axford, and J. Zeidler. The performance of adaptive equalization for digital communications systems corrupted by interference. In *27th ASILOMAR Conf. on Signals, Systems and Computers*, pages 1548–1553, 1993.

[14] M. Reuter and R. North. Manuscript in preparation.